Contrib. Astron. Obs. Skalnaté Pleso **50**, 96 – 104, (2020)
https://doi.org/10.31577/caosp.2020.50.1.96

Hydrogen Balmer spectral lines in spectroscopy of underwater electric spark discharge plasma

A. Murmantsev[1], **A. Veklich**[1], **V. Boretskij**[1] **and K. Lopatko**[2]

[1] *Taras Shevchenko National University of Kiev, 63/13, Volodymyrska str., Kyiv 01601, Ukraine*

[2] *National University of Life and Environmental Sciences of Ukraine, Kyiv, Ukraine*

Received: July 31, 2019; Accepted: December 2, 2019

Abstract. The behavior of the Balmer series spectral line profiles in the underwater electric spark discharge plasma between copper granules is investigated. Specially developed pulse power source is used to initiate a discharge between copper granules immersed into the deionized water. Typical values of voltage are of 40 – 200 V, current is up to 600 A and pulse frequency is in the range of 0.2 – 2 kHz. The voltage, applied to electrodes, caused a current flow along the chain of closely arranged granules in the stochastic switching mode. Optical emission spectroscopy methods are used for diagnostics of such discharge plasma. Profiles of $H\alpha$ and $H\beta$ hydrogen lines, exposed to the Stark mechanism of spectral lines' broadening, are used to determine electron density. The Boltzmann plot of copper lines' intensities are used to determine the plasma temperature.

Key words: underwater spark discharge – Boltzmann plot – Balmer lines – profiles – Stark broadening

1. Introduction

The investigation of underwater discharge plasma is of great interest to scientists because of its practical use in biology and electrochemistry. This discharge is used as a high-efficient method for the water treatment, surface treatment and plasma sterilizations (Babaeva & Kushner, 2008; Bruggeman & Leys, 2009; Clements et al., 1987). Underwater discharge is widely used for synthesis of micro- and nanoparticles (Lopatko et al., 2015; Cressault et al., 2013). It was found that colloidal solutions with nanoparticles are the most suitable form for biological usage (Lopatko et al., 2009). It is known that the solutions of silver and copper nanoparticles have bactericidal, antiviral, antifungal and antiseptic effects (Xiu et al., 2012), what makes them essential biocide products.

Unfortunately, nowadays there is no exact physical model of such underwater discharge, which increases the interest in studying it, improving of dynamic process in discharge and optimization of generation of colloidal substance process. For improvement of these discharge characteristic and increase quality of

the output solution, it is important to understand main discharge plasma parameters, such as excitation temperature and electron density. Optical emission spectroscopy (OES) is one of the most common methods for determination of these parameters. Specifically, copper and hydrogen spectral lines are widely used for it. Cu I spectral lines are well-studied and widely used (usually Cu I 515.3 nm, broadened by quadratic Stark effect Konjević & Konjević 1986) for electron density measurements (Babich et al., 2014; Fesenko et al., 2014; Venger et al., 2017) as well as Hydrogen lines (Venger et al., 2017; Nikiforov et al., 2015; Wang et al., 2019; Jovičević et al., 2004).

In previous work the $H\alpha$ shape was studied in underwater spark discharge (Tmenova et al., 2017) and in underwater arc discharge with $H\beta$ spectral line (Venger et al., 2017). Electron density, obtained in Venger et al. (2017) from the width of $Cu\,I$ 515.3 nm and $H\alpha$ spectral lines were of the same order of magnitude for all the studied power modes, values of N_e, obtained from the width of $H\beta$ line were by two orders of magnitude lower for the cases of arc current of 660 and 800 A, and by one order of magnitude lower for the case of 1000 A. It aroused interest to study the behavior of $H\beta$ spectral line profile in underwater spark discharge.

Thus, the main goals of the presented work are investigation of Balmer spectral lines behavior in underwater electric spark discharge, determination of electron density and excitation temperature from $Cu\,I$ and $H\alpha$ spectral line profile as well as enrolment of $H\beta$ spectral line to electron density measurements by OES. It should give additional methods for future investigation of underwater spark discharge to find correlation of discharge plasma parameters and properties of colloidal substance.

2. Experimental setup

Specially developed pulse power source was used to initiate a discharge between copper granules immersed into the deionized water. Implementation of the low-voltage spark discharges was carried out on the experimental setup, which is shown in Fig.1. It consists of a pulse generator 1, control unit 2, measuring and auxiliary devices: oscilloscope 3, Rogowsky coil 4, voltage divider 5; and discharge chamber 6.

The voltage, applied to electrodes, caused a current flow along the chain of closely arranged granules in the stochastic switching mode. Investigation of the influence of process variables on dispersion and morphology of the products of metal granules erosion during the formation of local spark discharges was carry out. It was performed by varying of electrical parameters of the discharge circuit.

It must be noted, the investigations were carried out in two modes, which differ by generation power. The higher power (second) mode, as it turn out, must be used due to the fact, that $H\beta$ was not observe or was comparable

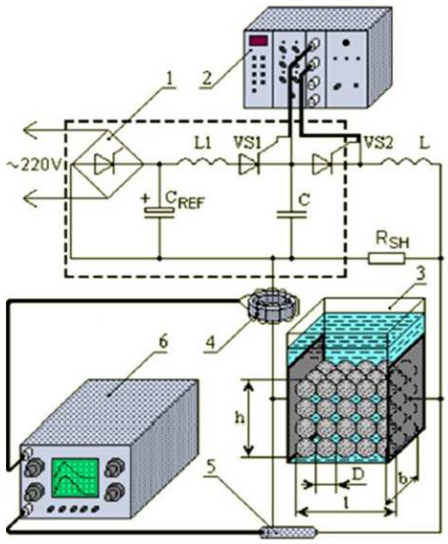

Figure 1. Scheme of experimental setup, that consists of a pulse generator 1, control unit 2, measuring and auxiliary devices: oscilloscope 3, Rogowsky coil 4, voltage divider 5; and discharge chamber 6.

with noise at lower power (first mode). Typical values of voltage were of 40 – 200 V, currents were 100 – 300 A in the first mode and 400 – 600 A in the second mode and pulse frequency was in the range of 0.2 – 2 kHz. As a result of a spark-erosion process, the formation of colloidal fraction was observed. Its morphology markedly differs from a micro fraction and is a common for metallurgical processes at low pressure, namely, the formation of a solid phase resulting from evaporation followed by condensation.

Spectra with Balmer and copper spectral lines were registered by Solar LS SDH-IV spectrometer with a 4-position manually switchable diffraction gratings turret in this investigation. Spectra were registered by CCD (Toshiba TCD 1304 AP, 3648 px). Two spectrometer ranges in two different modes were used to extend the studied spectral range. The first mode was realized in spectral range of 450-910 nm with 0.09 nm spectral resolution, the second mode - in 290-610 nm with 0.18 nm spectral resolution. Spectral sensitivity of this device was determined by tungsten band-lamp and was taken into account in spectral data treatment.

3. Results and Discussions

Fig.2a and 2b show spectra with marked spectral lines, registered in the first and second modes, correspondingly.

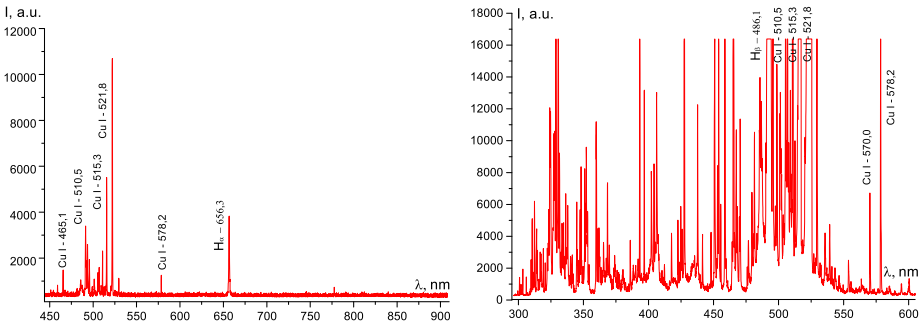

a) b)

Figure 2. Registered spectra: (a) - the first mode; (b) - the second mode.

The electron density in plasma at the first mode was obtained from the width of $Cu\,I$ 515.3 nm and $H\alpha$ spectral lines. The Voigt function was used in this study to account for spectrometer instrument function, as well as, to determine the Stark width (see Fig.3a and 3b). Other broadened mechanisms (such as resonance broadening, van der Waals broadening etc.) were neglected in this study e.g. (Nikiforov et al., 2015; Laux et al., 2003; Marinov et al., 2014).

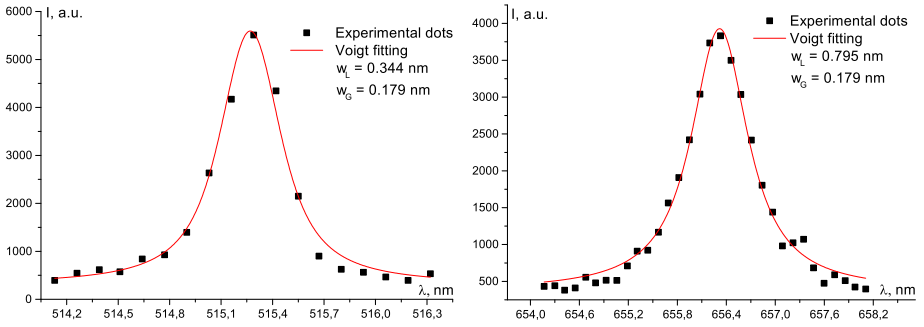

a) b)

Figure 3. Voigt fitting of spectral line profile of: (a) - Cu I 515.3 nm; (b) - $H\alpha$ 656.3 nm.

Electron density, obtained from the widths of $Cu\,I$ 515.3 nm and $H\alpha$ spectral lines, was of $9.9\times10^{16}\ cm^{-3}$ and $6.7\times10^{16}\ cm^{-3}$, respectively. Plasma excitation temperature was determined by Boltzmann plot technique. Fig.4 shows typical

Boltzmann plot, obtained by $Cu\,I$ 465.1, 510.5, 515.3, 521.8 and 578.2 nm spectral lines. It was found from this plot, that excitation temperature in thise plasma source was of $10500 \pm 900\,K$.

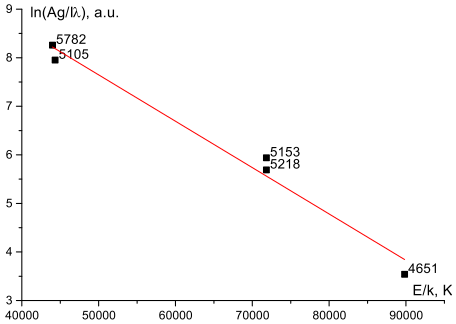

Figure 4. Boltzmann plot on the base of Cu I spectral lines.

As one can see from Fig.2b, the spectrum becomes very complicated at the second mode and a lot of spectral lines were exposed. The use of $Cu\,I$ 515.3 nm spectral line was not possible, since it went beyond of the CCD dynamic range. That is why the $Cu\,I$ 570.0 nm, in assumption that it broadened by quadratic Stark effect (Konjević & Konjević (1986)), and $H\beta$ spectral lines were used for electron density measurements (see Fig.5a and 5b). $H\alpha$ (656.3 nm) spectral line was not registered in this mode due to limited spectral range (290-610 nm).

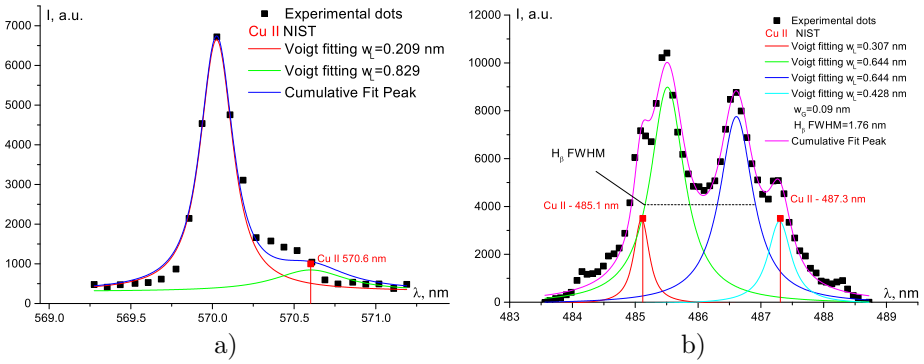

Figure 5. Voigt fitting of spectral line profile of: (a) - Cu I 570.0 nm; (b) - $H\beta$ 486.1 nm.

$H\beta$ was approximated by four peaks Voigt profile (Fig.5a) due to two reasons. Firstly, this line had complex shape, specifically, it had dip in the center of line. Secondly, it was overlapped by $Cu\,II$ 485.1 and 487.3 nm spectral lines.

In a similar way it was taken into account (by two peaks Voigt profile) the overlapping of $Cu\,I$ 570.0 nm and $Cu\,II$ 570.6 nm spectral lines (Fig.5b).

The electron density, obtained from $H\beta$ width, can be determined in accordance with Konjević et al. (2012):

$$N_e[m^{-3}] = 10^{22} * (w_S[nm]/0.94666)^{1.49}, \tag{1}$$

where w_S is a Stark width. It must be noted, that w_S not equal width of Lorentz part of the Voigt function (w_L) (Konjević et al., 2012) and must be determined in accordance with Kelleher (1981):

$$w_S = (w_M^{1.4} - w_{D,I}^{1.4})^{1/1.4}, \tag{2}$$

where w_M is the measured FWHM, $w_{D,I}^2 = w_D^2 + w_I^2$ (w_D - Doppler width, w_I - width of instrument function).

The value of electron density, obtained from $H\beta$ width was of $1.73{\times}10^{16}\,cm^{-3}$, from $Cu\,I$ 570.0 nm width - $6.92 \times 10^{17}\,cm^{-3}$.

As one can see, electron density values, obtained from width of $Cu\,I$ 515.3 nm and $H\alpha$ spectral lines are of the same order of magnitude. As for $H\beta$ spectral line, electron density value, obtained from the width of this line is by one order of magnitude lower in comparison of value, obtained from the width of $Cu\,I$ 570.0 nm spectral line. That is the similar results, obtained in previous work (Venger et al., 2017) and, obviously, must be as a subject of future investigation.

The impact of other broadening mechanisms were estimated on base of experimentally obtained plasma parameters (temperature and electron density) to testify the aforementioned neglection. The relations showed by Griem (1974) were used.

Van der Waals broadening. Calculations of van der Waals widths were carry out for different perturbers, specifically, for H, O and Cu. It was assumed that the temperature is 1 eV for the second mode, electron density provided predominantly by copper atoms. Concentrations of such atoms were calculated by Saha equation and were $7 \times 10^{15}\,cm^{-3}$ and $2 \times 10^{17}\,cm^{-3}$ for the first and the second modes, respectively. The ratios between intensities of Cu and H lines were found from the spectra (see Fig.2) to calculate the concentration of Hydrogen atoms of $4 \times 10^{18}\,cm^{-3}$ and $8 \times 10^{18}\,cm^{-3}$ for the first and the second modes, respectively. Polarizability of H and O was taken from Allen (1976), and for Cu, it was taken from Sarkisov et al. (2019). It was estimated that maximal value of van der Waals width was 0.03 nm for $H\alpha$ spectral line with Cu as a perturber.

Resonance broadening. The values of resonance broadening width were lower than 0.003 nm for copper spectral lines and lower than 0.002 nm for Balmer lines.

The values of resonance and van der Waals broadening are much lower than observed line widths, which confirms neglection of other mechanisms except Stark broadening.

Optical Thickness of plasma was estimated additionally. The opacities for different spectral lines were calculated in assumption of the Boltzmann distribu-

tion of atom energy level population. The value of optical thickness for $H\alpha$, $H\beta$ and $Cu\,I$ 570.0 nm spectral lines were 0.02, 0.004 and 0.006 respectively. The plasma radii were assumed of 1 mm in this case. These results give the reason to disregard the contribution of opacity in data treatment.

4. Conclusions

The behavior of Balmer spectral line profiles, in particulary, $H\alpha$ and $H\beta$ was investigated. OES was used for determination of excitation temperature and electron density in plasma of underwater spark discharge.

The values of electron density at lower power mode, obtained from widths of $H\alpha$ and $Cu\,I$ 515.3 nm spectral lines are the same in order of magnitude. In contrast to this, in the second mode, $H\beta$ and $Cu\,I$ 570.0 nm spectral lines give different results of electron density which is coincide with behavior, observed in previous experiment.

Presently, on the one hand, it is impossible to talk about aptitude of electron density measurements in plasma of underwater spark discharge from the $H\beta$ spectral line profile. On the other hand, such method can be considered potential for such aims. Thus, such investigation should be continued and implemented in other ways in future studies.

References

Allen, C. W. 1976, *Astrophysical Quantities*

Babaeva, N. & Kushner, M., Streamer Branching: The Role of Inhomogeneities and Bubbles. 2008, *IEEE Trans. Plasma Sci.*, **38**, 892, DOI: 10.1109/TPS.2008.922434

Babich, I. L., Boretskij, V. F., Veklich, A. N., & Semenyshyn, R. V., Spectroscopic data and Stark broadening of Cu I and Ag I spectral lines: Selection and analysis. 2014, *Adv. Space Res.*, **54**, 1254, DOI: 10.1016/j.asr.2013.10.034

Bruggeman, P. & Leys, C., TOPICAL REVIEW: Non-thermal plasmas in and in contact with liquids. 2009, *J. Ph. D. Appl. Phys.*, **42**, 053001, DOI: 10.1088/0022-3727/42/5/053001

Clements, J., Sato, M., & Davis, R., Preliminary investigation of prebreakdown phenomena and chemicalreactions using a pulsed high-voltage discharge in water. 1987, *IEEE Trans. Ind. Appl.*, **23**, 224, DOI: 10.1109/TIA.1987.4504897

Cressault, Y., Teulet, P., Gleizes, A., et al., Peculiarities of metal nanoparticles generation by underwater discharges for biological applications. 2013, in XXXIth International Conference on Phenomena in Ionized Gases, Vol. **1**, , 14–19

Fesenko, S., Veklich, A., Boretskij, V., et al., Properties of thermal air plasma with admixing of copper and carbon. 2014, in Journal of Physics Conference Series, Vol. **550**, *J. Phys. Conference Series*, 012008

Griem, H. R. 1974, *Spectral line broadening by plasmas*

Jovičević, S., Ivković, M., Konjević, N., Popović, S., & Vušković, L., Excessive Balmer line broadening in microwave-induced discharges. 2004, *J. Appl. Phys.*, **95**, 24, DOI: 10.1063/1.1629133

Kelleher, D., Stark broadening of visible neutral helium lines in a plasma. 1981, *J. Quant. Spectrosc. Radiat. Transfer*, **25**, 191, DOI: https://doi.org/10.1016/0022-4073(81)90089-3

Konjević, N., Ivković, M., & Sakan, N., Hydrogen Balmer lines for low electron number density plasma diagnostics. 2012, *Spectrochimica Acta*, **76**, 16, DOI: 10.1016/j.sab.2012.06.026

Konjević, R. & Konjević, N., Stark broadening and shift of neutral copper spectral lines. 1986, *Fizika*, **18**, 327

Laux, C. O., Spence, T. G., Kruger, C. H., & Zare, R. N., Optical diagnostics of atmospheric pressure air plasmas. 2003, *Plasma Sources Science Technology*, **12**, 125, DOI: 10.1088/0963-0252/12/2/301

Lopatko, K., Aftandiliants, Y., & Kalenska, S., Colloidal Solution of Metal. 2009, *Ukrainian Patent*, 12

Lopatko, K., Aftandiliants, Y., Veklich, A., et al., Enrichment of colloidal solutions by nanoparticles in underwater spark discharge. 2015, *Probs. At. Sci. and Tech.*, **10**, 267

Marinov, I., Starikovskaia, S., & Rousseau, A., Dynamics of plasma evolution in a nanosecond underwater discharge. 2014, *Journal of Physics D Applied Physics*, **47**, 224017, DOI: 10.1088/0022-3727/47/22/224017

Nikiforov, A. Y., Leys, C., Gonzalez, M. A., & Walsh, J. L., Electron density measurement in atmospheric pressure plasma jets: Stark broadening of hydrogenated and non-hydrogenated lines. 2015, *Plasma Sources Science Technology*, **24**, 034001, DOI: 10.1088/0963-0252/24/3/034001

Sarkisov, G. S., Hamilton, A., & Sotnikov, V., Dynamic dipole polarizability of gold and copper atoms for 532- and 1064-nm wavelengths. 2019, *Phys. Rev. A*, **99**, 012503, DOI: 10.1103/PhysRevA.99.012503

Tmenova, T., Veklich, A., Boretskij, V., et al., Optical emission spectroscopy of plasma of underwater electric spark discharge between metal granules. 2017, *Probs. At. Sci. and Tech.*, **107**, 132

Venger, R., Tmenova, T., Valensi, F., et al., Detailed Investigation of the Electric Discharge Plasma between Copper Electrodes Immersed into Water. 2017, *Atoms*, **5**, 40, DOI: 10.3390/atoms5040040

Wang, H., Wandell, R. J., Tachibana, K., Voráč, J., & Locke, B. R., The influence of liquid conductivity on electrical breakdown and hydrogen peroxide production in a nanosecond pulsed plasma discharge generated in a water-film plasma reactor. 2019, *J. Phys. D. Appl. Phys.*, **52**, 075201, DOI: 10.1088/1361-6463/aaf132

Xiu, Z.-m., Zhang, Q.-b., Puppala, H. L., Colvin, V. L., & Alvarez, P. J. J., Negligible Particle-Specific Antibacterial Activity of Silver Nanoparticles. 2012, *Nano Letters*, **12**, 4271, DOI: 10.1021/nl301934w